Electronic Supplementary Information

Investigation of protein/DNA binding, and *in vitro* cytotoxicity of novel Cu (II) and Zn(II)-dipyrazinyl pyridine complexes

Parnashabari Sarkar,[a] Munmi Gogoi,[b] Sonali Palo,[a] A.H. Udaya Kumar,[c] Sourav Sutradhar,[a] Dipankar Das,[a] N.K. Lokanath,[c] Akalesh Kumar Verma,*[b] Biswa Nath Ghosh*[a]

[a]*Department of Chemistry, National Institute of Technology Silchar, Silchar-788010, Assam, India,* bnghosh@che.nits.ac.in

[b]*Department of Zoology, Cell & Biochemical Technology Laboratory, Cotton University, Guwahati-781001, Assam, India,* akhilesh@cottonuniversity.ac.in

[c]*Department of Studies in Physics, University of Mysore, Manasagangotri, Mysuru 570 006, Karnataka, India*

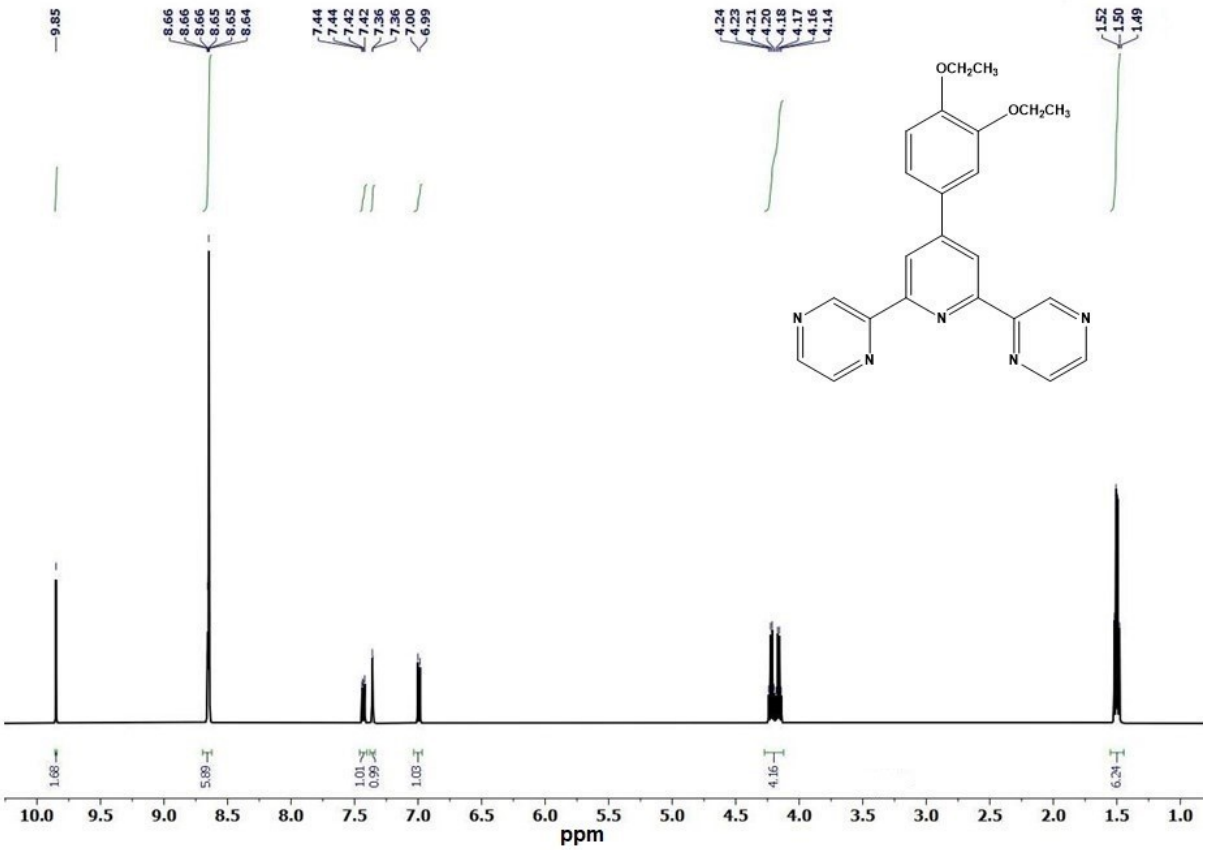

Figure S1(a): 400 MHz ^{1}H NMR spectrum of **L** in $CDCl_3$.

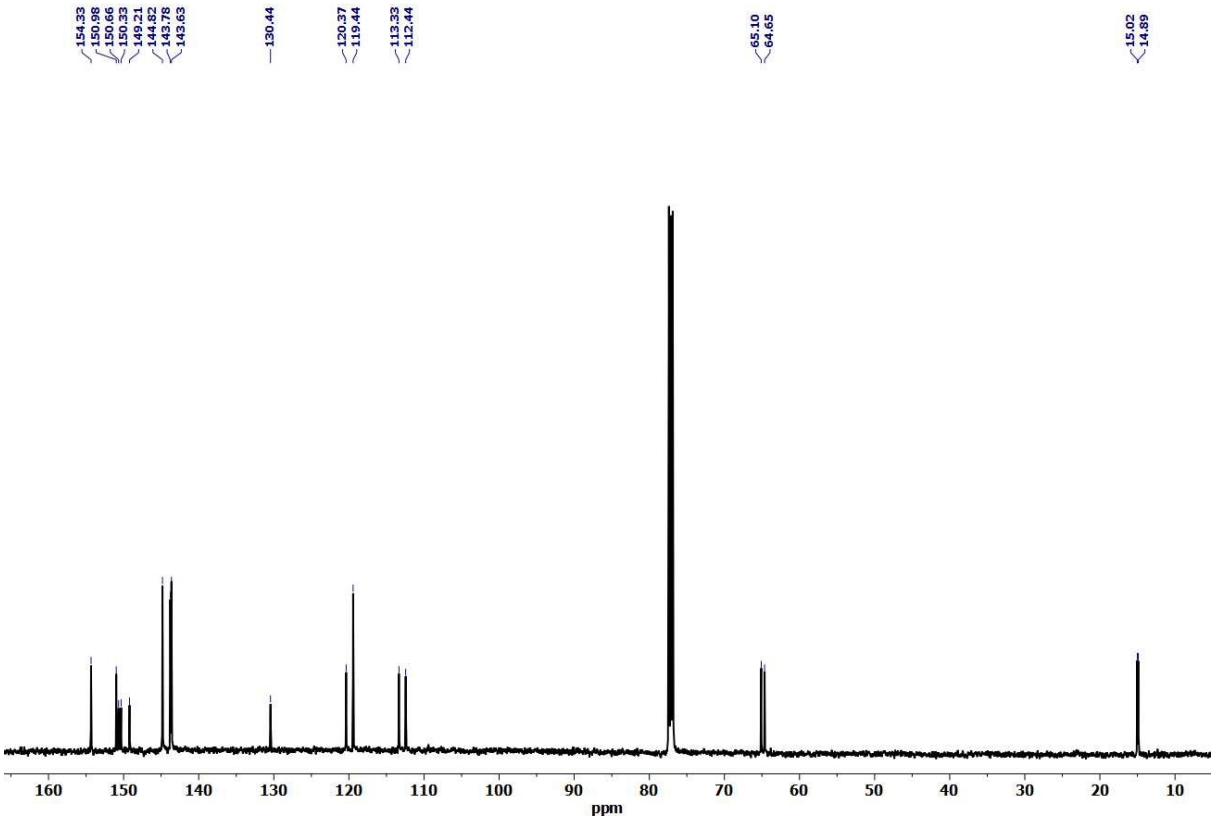

Figure S1(b): 125 MHz ^{13}C NMR spectrum of **L** in $CDCl_3$.

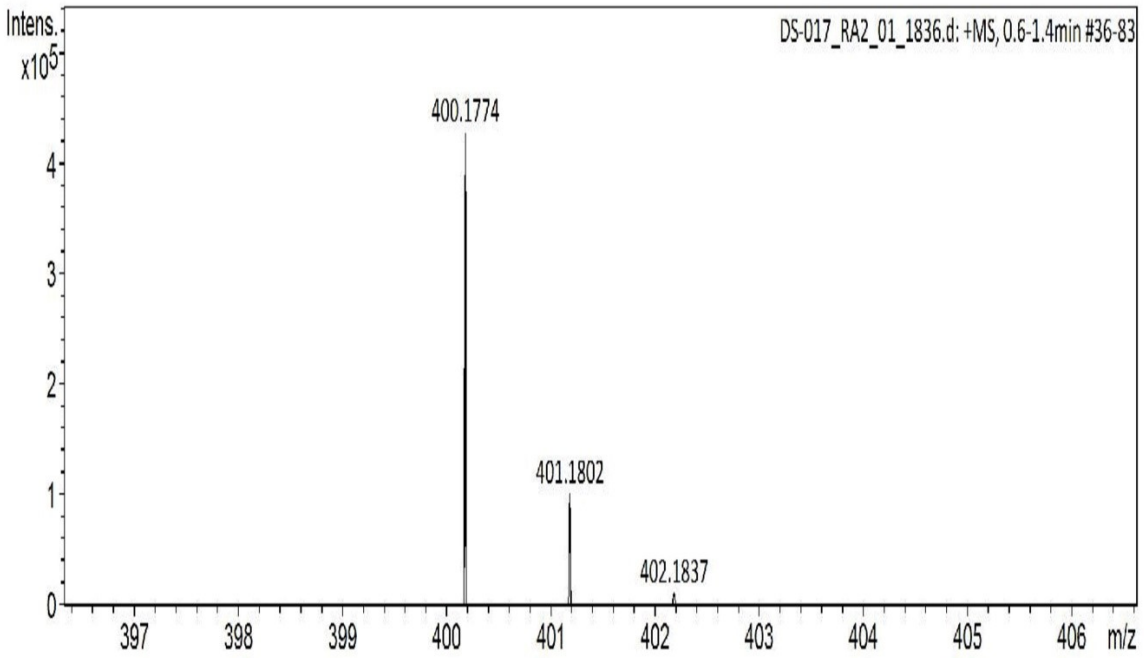

Figure S1(c): ESI-MS spectrum of **L** in $CDCl_3$.

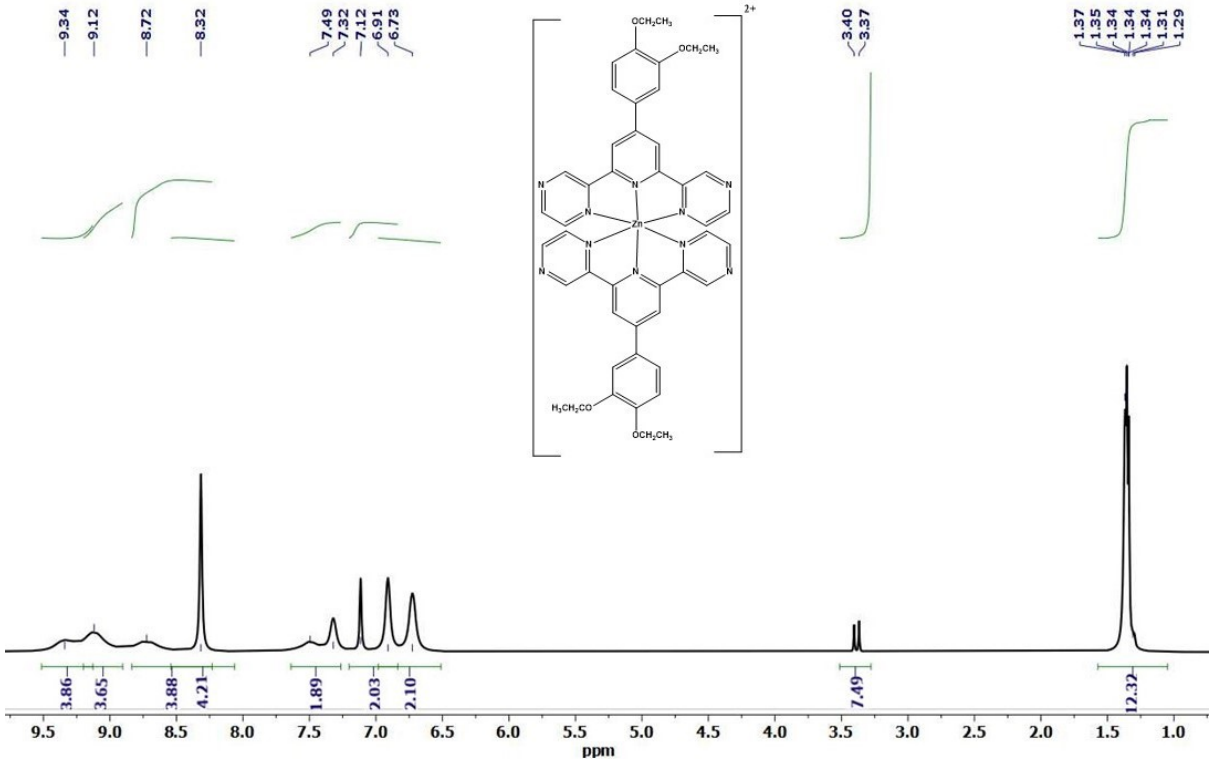

Figure S2: 400 MHz ^{1}H NMR spectrum of **2** in DMSO-d6.

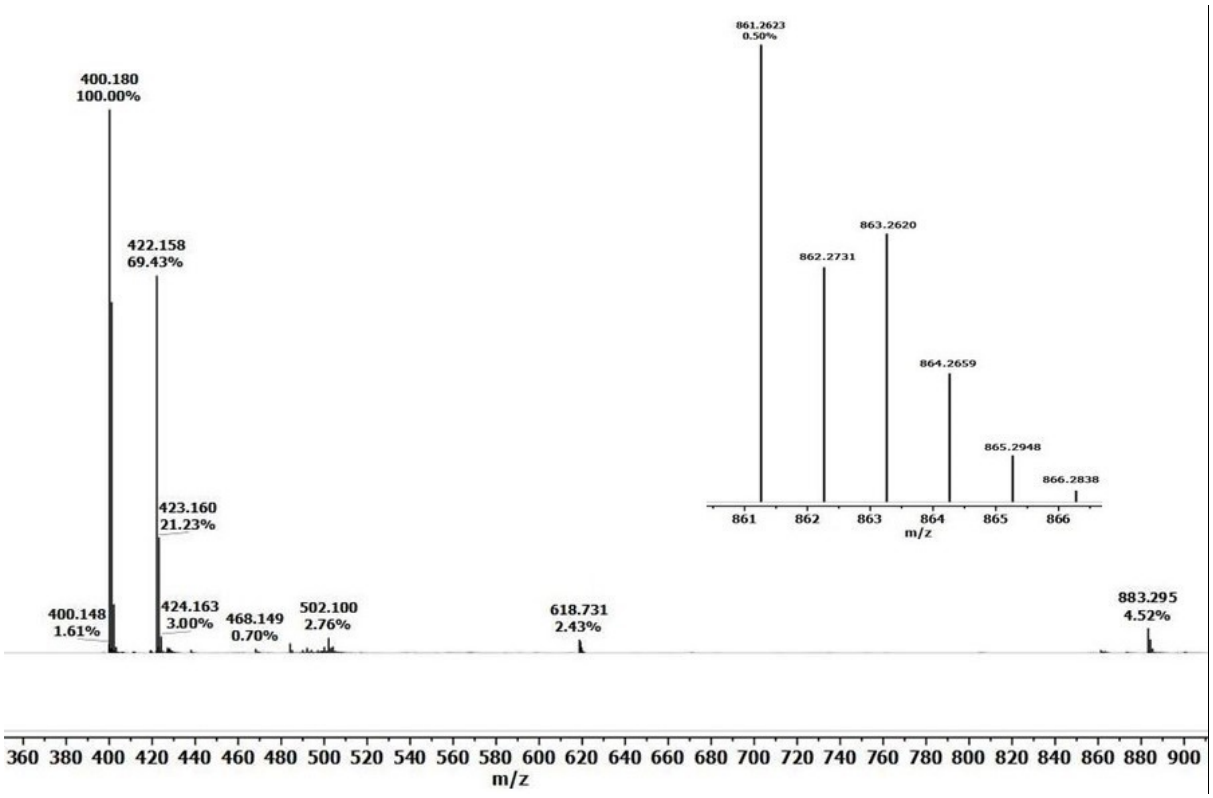

Figure S3: HR-MS of Cu (II) complex **1** (Inset: Isotopic distribution of molecular ion peak) inset).

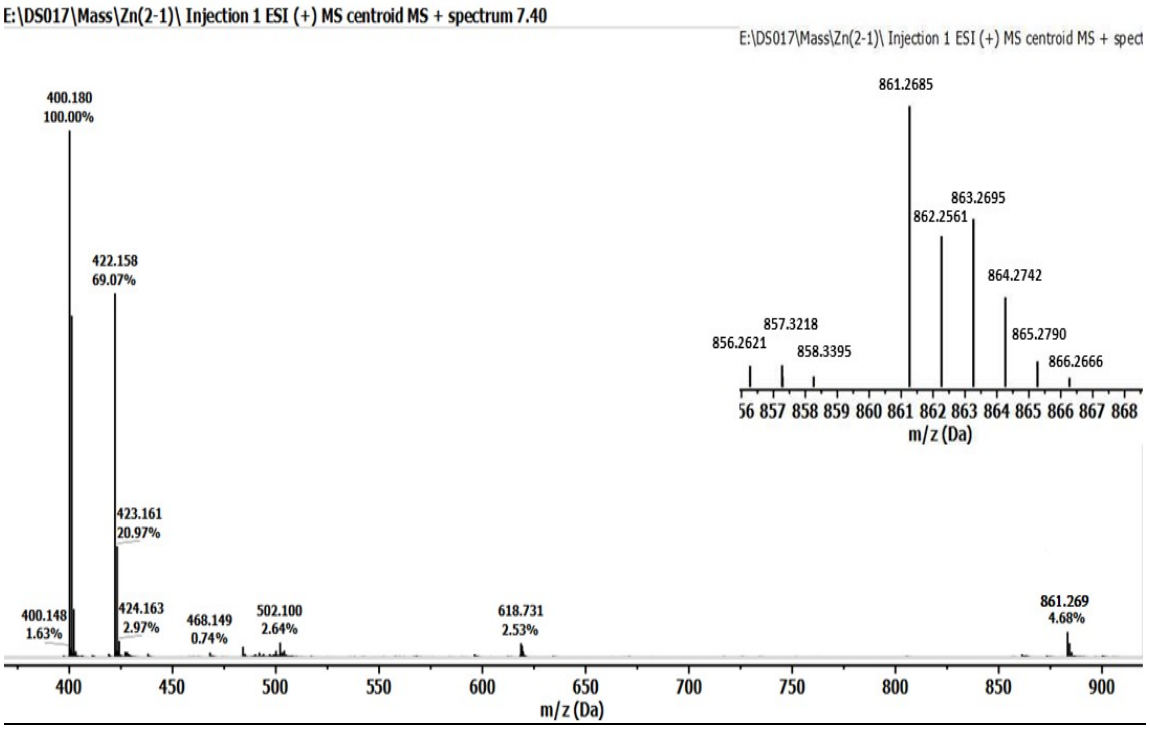

Figure S4: HR-MS of Zn (II) complex **2**. (Inset: Isotopic distribution of molecular ion peak)

Thermal stabilities of complexes

Thermal stabilities of complexes **1** and **2** have been investigated under the N_2 atmosphere by TGA at a 30-700 °C temperature range, with a heating rate of 10 °C/min. The thermal decomposition of the complexes take place with two main weight loss steps. The first weight loss starts from 30 °C to 330 °C in the DTG curve, attributed to the release of counter anion chloride (obs. 7.4% (for **1**) and 6.7% (for **2**), cal. 7.5% (for both **1-2**)). The second decomposition processes occur in the temperature range of 285-420 °C. The corresponding endothermic peaks are observed in the DTG curve at 390 °C for **1** (obs. 58.75%, cal. 53.68% for **1**) and 400 °C for **2** (obs. 57.88%, cal. 53.81% for **1**), corresponding to the loss of Cu(dppy) and Zn(dppy) fragment.

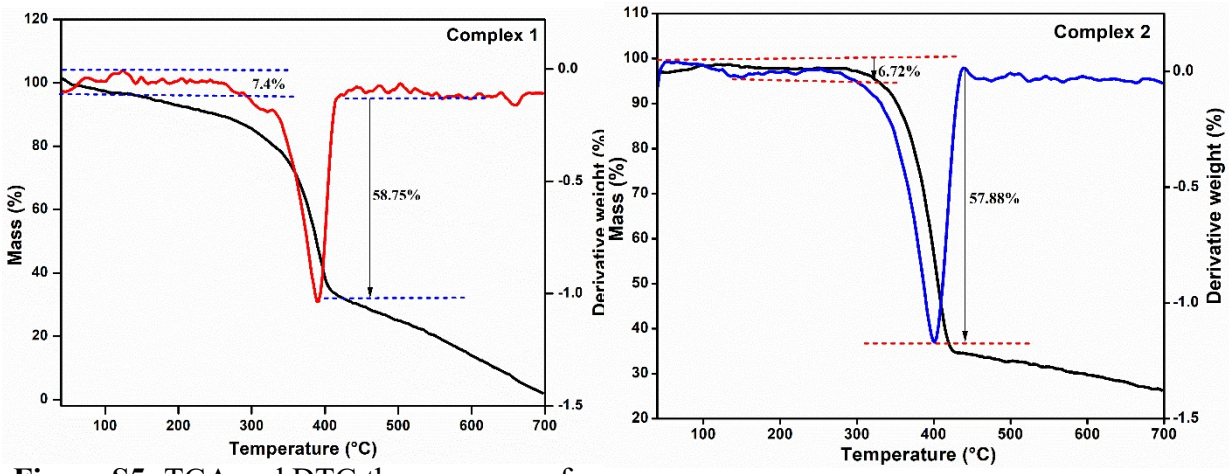

Figure S5: TGA and DTG thermograms of complexes **1** (left) and **2** (right)

Table S1. Second-order perturbation theory analysis of Fock matrix in NBO calculation for **L**

	Donor (i)	Type	Occupancy	Acceptor(j)	Type	Occupancy	E(2) kcal/mol	E(j)-E(i) a.u	F(i, j) a.u
ligand	C9-N32	π*	0.40233	C7-C8	π*	0.34499	293.8	0.01	0.084
	C9-N32	π*	0.40233	C10-C11	π*	0.32966	250.39	0.01	0.081
	C2-C3	π*	0.38227	C1-C6	π*	0.38115	246.21	0.01	0.08

	C17-N33	π*	0.34302	C18-C19	π*	0.31103	166.23	0.02	0.08
	C7-C8	π*	0.34499	C1-C6	π*	0.38115	125.57	0.01	0.054
	C20-N51	π*	0.36362	C18-C19	π*	0.31103	120.94	0.02	0.079
	C27	LP(1)	0.94676	C26-N50	π*	0.35578	88.71	0.12	0.112
	C25	LP*(1)	0.94087	C24-N34	π*	0.3417	77.9	0.13	0.112
	C27	LP(1)	0.94676	C24-N34	π*	0.3417	70.41	0.12	0.103
	C25	LP*(1)	0.94087	C26-N50	π*	0.3417	68.96	0.12	0.103

Table S2: Second-order perturbation theory analysis of Fock matrix in NBO calculation for complexes **1** and **2**.

	Donor (i)	Type	Occupancy	Acceptor(j)	Type	Occupancy	E(2) kcal/mol	E(j)-E(i) a.u	F(i, j) a.u
Complex **2**	C56-C61	π*	0.18746	C41-C55	π*	0.20044	139.96	0.01	0.079
	C58-C65	π*	0.18935	C54-C57	π*	0.19912	135.05	0.01	0.079
	C59-C67	π*	0.1952	C41-C55	π*	0.20044	127.26	0.01	0.081
	C63-C70	π*	0.1965	C54-C57	π*	0.19912	124.9	0.01	0.081
	N8-C12	π*	0.34714	C25-N42	π*	0.1668	123.33	0.02	0.096
	C19	LP(1)	0.52265	N2-C9	π*	0.37942	68.49	0.1	0.108
	N2-C9	π*	0.37942	C21-C38	π*	0.19422	63.09	0.06	0.099
	N1-C3	π*	0.38106	C11-C23	π*	0.19091	61.8	0.06	0.099
	C21-C38	π*	0.19422	C54-C57	π*	0.19912	60.96	0.01	0.06
	C11-C23	π*	0.19091	C41-C55	π*	0.20044	57.03	0.01	0.058
Complex **1**	C58-C65	π*	1.97757	C54-C57	π*	0.39507	277.56	0.01	0.079
	N6-C17	π*	1.65183	C32-N47	π*	0.3378	255.42	0.02	0.094
	C63-C70	π*	1.65183	C54-C57	π*	0.39507	255.34	0.01	0.081
	N8-C12	π*	1.97752	C25-N42	π*	0.33783	255.28	0.02	0.094

	N5-C14	π*	1.97203	C27-N44	π*	0.33749	253.71	0.02	0.094
	N7-C19	π*	1.97757	C35-N50	π*	0.33736	253	0.02	0.094
	C35-N50	π*	1.97203	C18-C33	π*	0.26457	86.98	0.02	0.071
	C27-N44	π*	1.9775	C15-C28	π*	0.2645	86.96	0.02	0.071
	C32-N47	π*	1.97207	C16-C30	π*	0.26456	85.68	0.02	0.071
	C25-N42	π*	1.97207	C20-C36	π*	0.26465	32.48	0.16	0.107

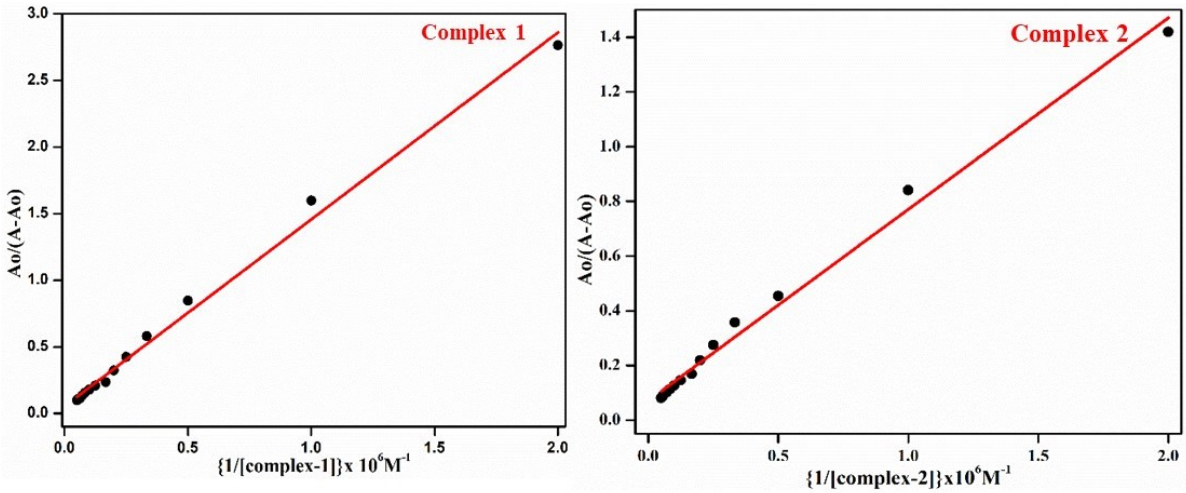

Figure S6: Benesi-Hildebrand plot $\{A_o/(A-A_o)$ vs. 1/[complex]} of absorption spectra of BSA in the absence and presence of complex **1** and complex **2**.

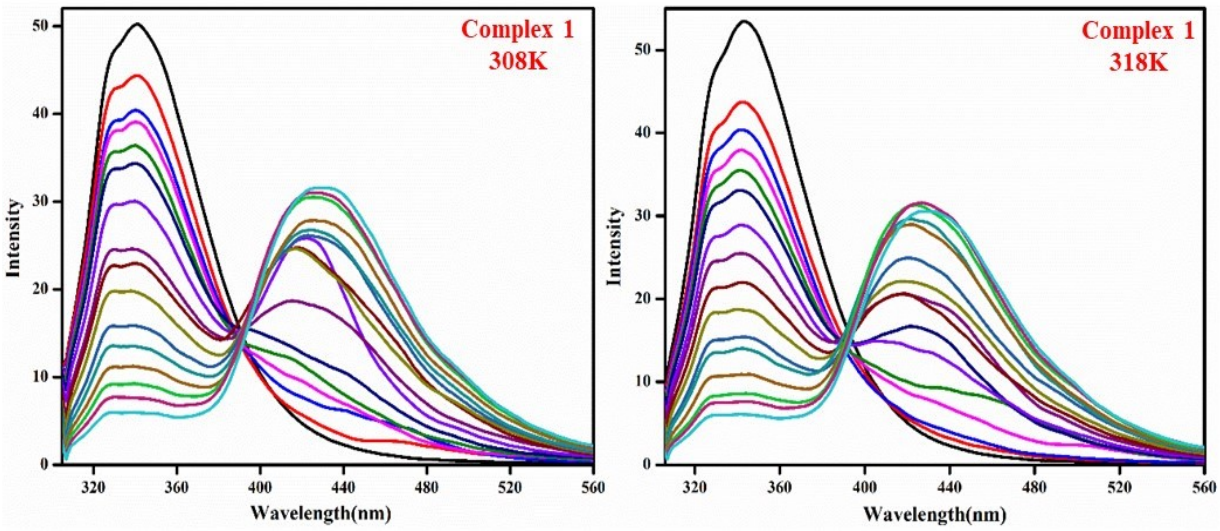

Figure S7: Emission spectra of BSA (10 μM) (λ_{ex} = 280 nm) in the presence of increasing concentrations of complex **1** at 308 K and 318 K.

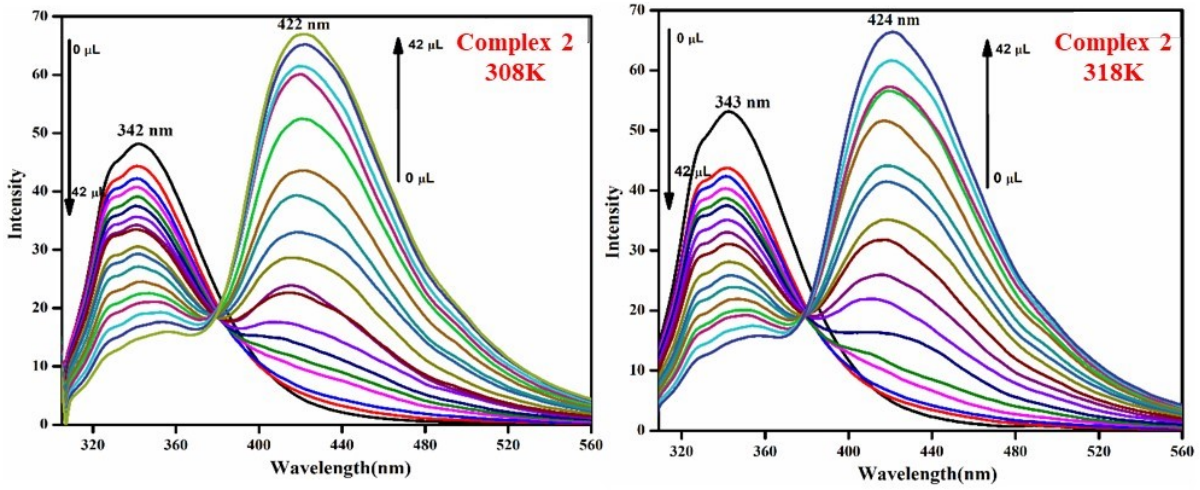

Figure S8: Emission spectra of BSA (10 μM) (λ_{ex} = 280 nm) in the presence of increasing concentrations of complex **2** at 308 K and 318 K.

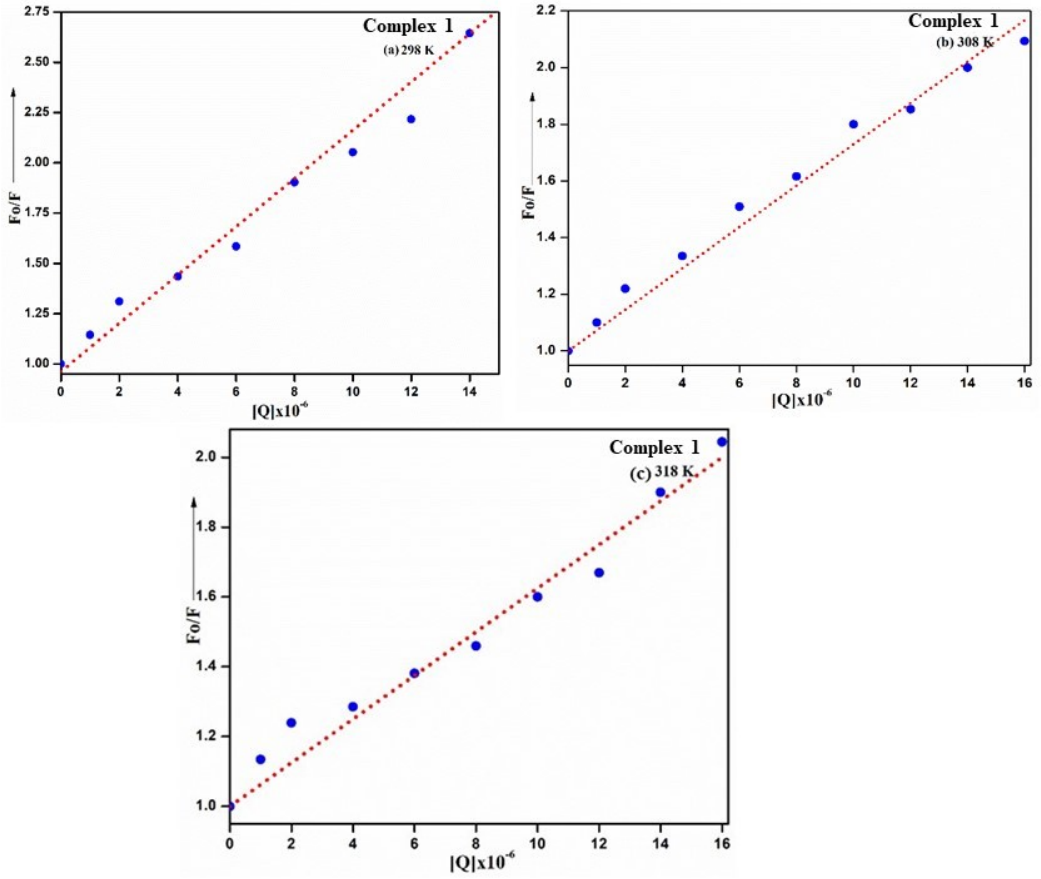

Figure S9: Stern-Volmer plot {F_0/F vs. [complex]} of emission spectra of BSA in the absence and presence of complex **1** at 298 K, 308 K and 318 K.

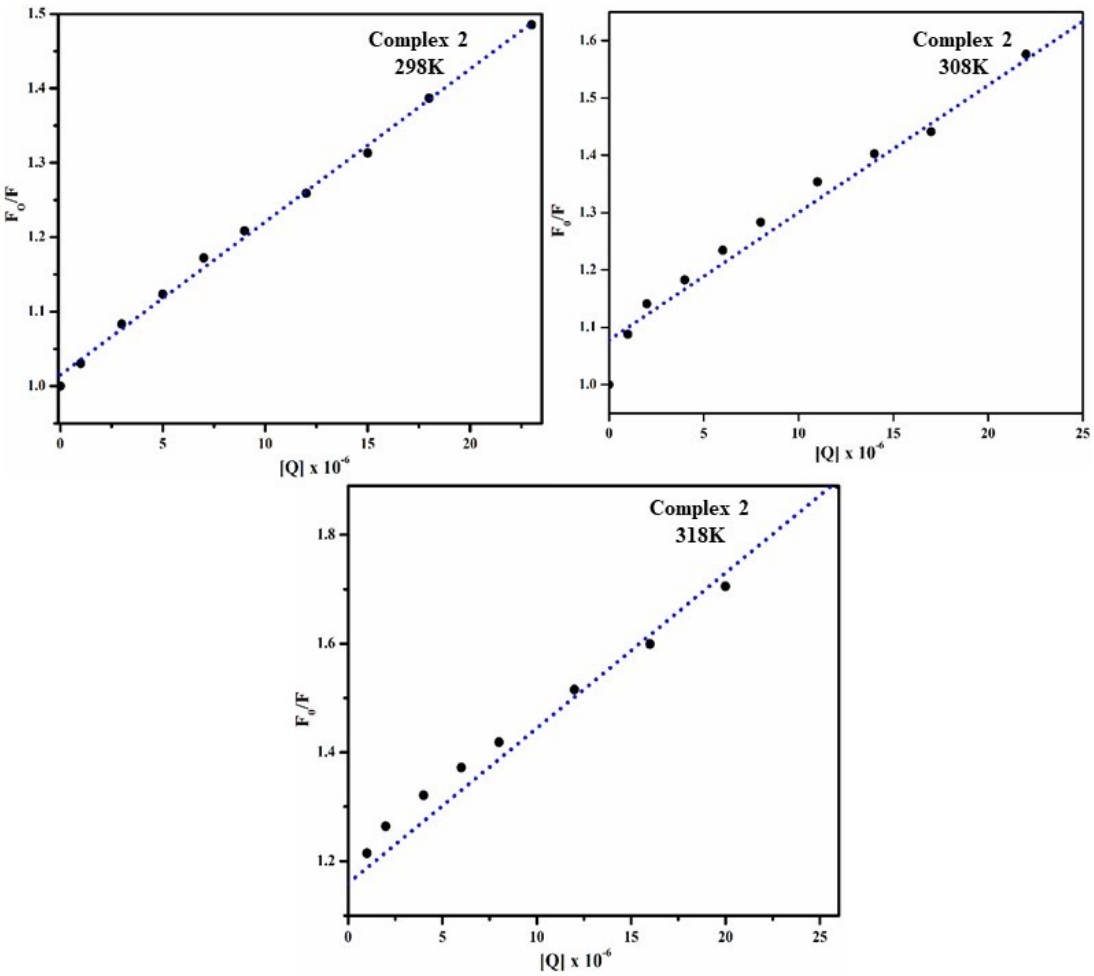

Figure S10: Stern-Volmer plot {F0/F vs. [complex]} of emission spectra of BSA in the absence and presence of complex **2** at 298 , 308 K, and 318 K.

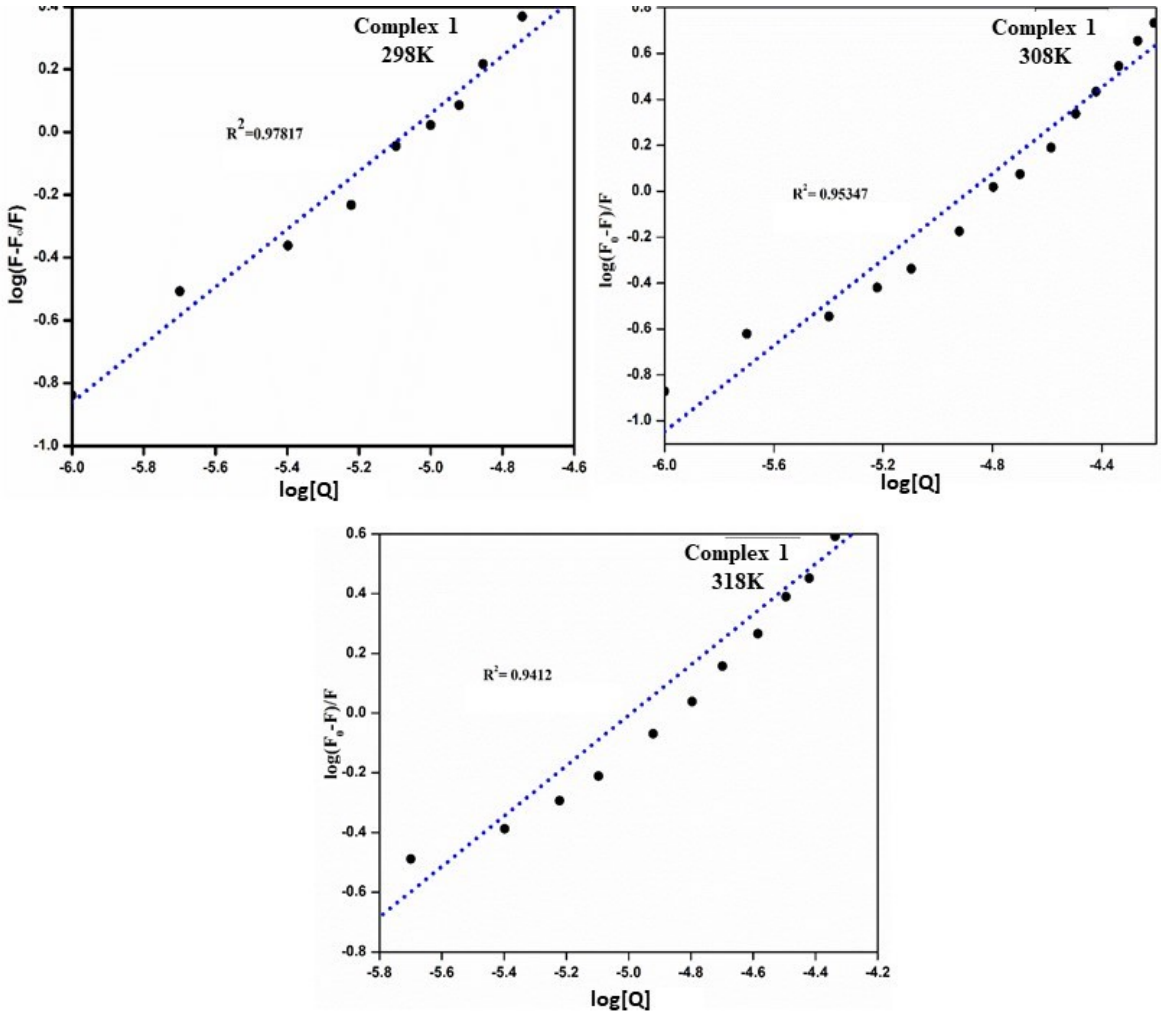

Figure S11: Modified Stern-Volmer plot of emission spectra of BSA in the absence and presence of complex **1** at 298 K, 308 K and 318 K.

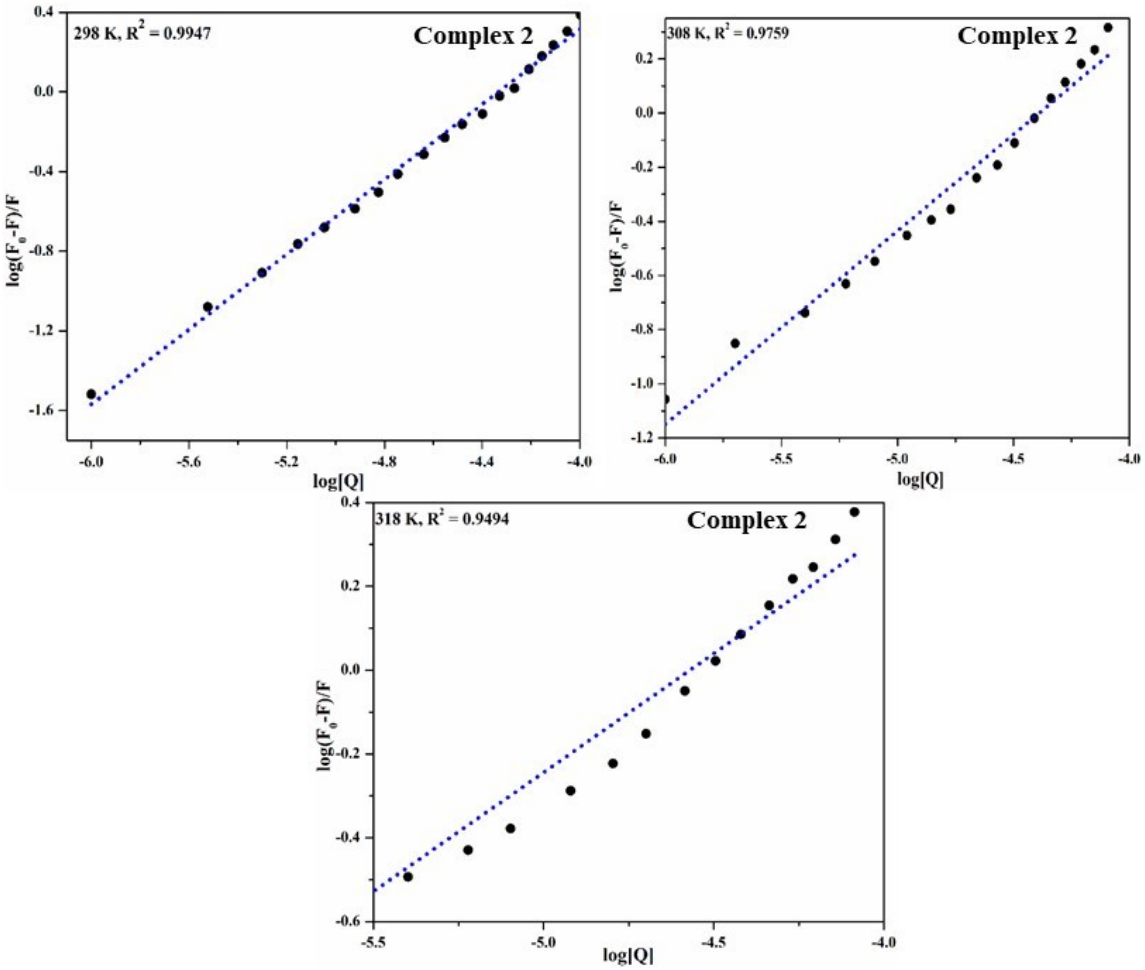

Figure S12: Modified Stern-Volmer plot of emission spectra of BSA in the absence and presence of complex **2** at 298 K, 308 K, and 318 K.

Equations **1-3** are employed to analyse thermodynamic parameters like ΔH, ΔG, and ΔS, if the enthalpy change (ΔH) does not vary much over the temperature range under study.

$$\ln K = \Delta H/RT + \Delta S/R \qquad (1)$$

$$\Delta G = -RT\ln K \qquad (2)$$

$$\Delta S = (\Delta H - \Delta G)/T \qquad (3)$$

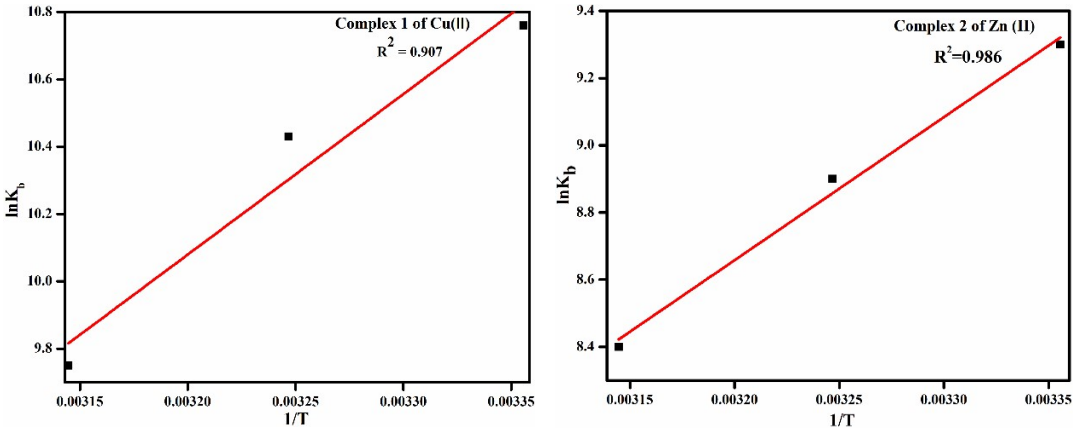

Figure S13: van't Hoff plots for BSA in presence of complexes **1** and **2** at different temperatures.

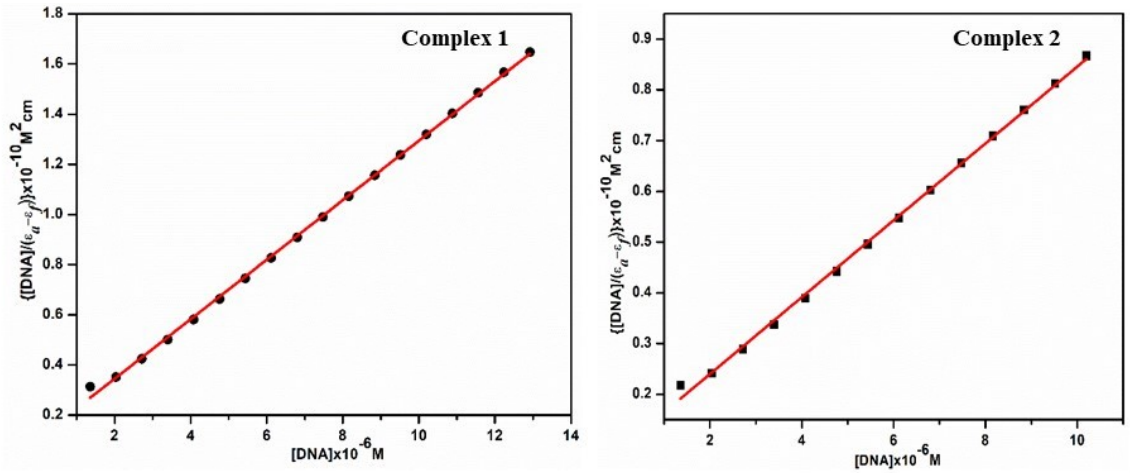

Figure S14: DNA binding study of metal complexes in the absence and presence of DNA with the electronic absorption spectra.

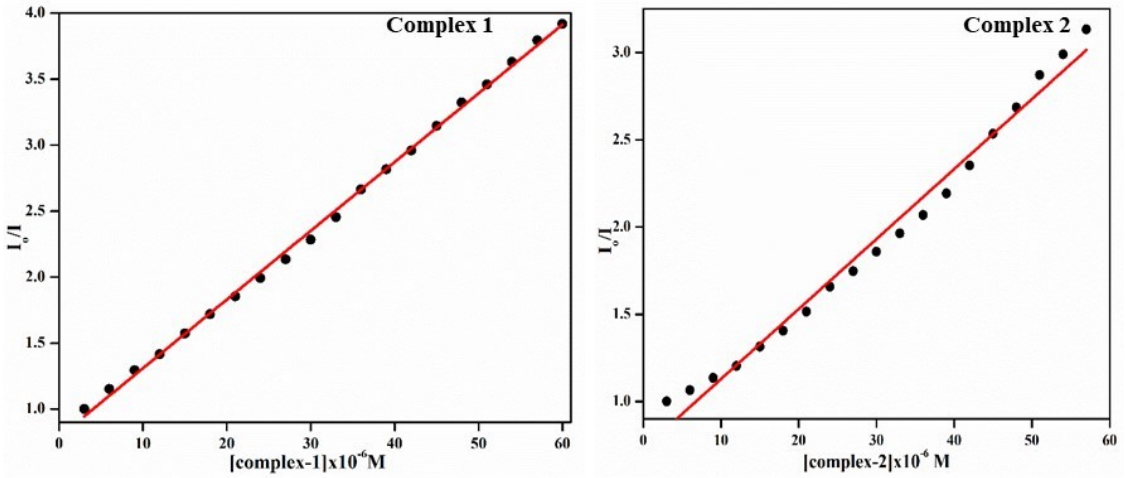

Figure S15: Stern-Volmer plot {F₀/F vs. [complex]} of emission spectra of DNA in the absence and presence of complex **1-2**.

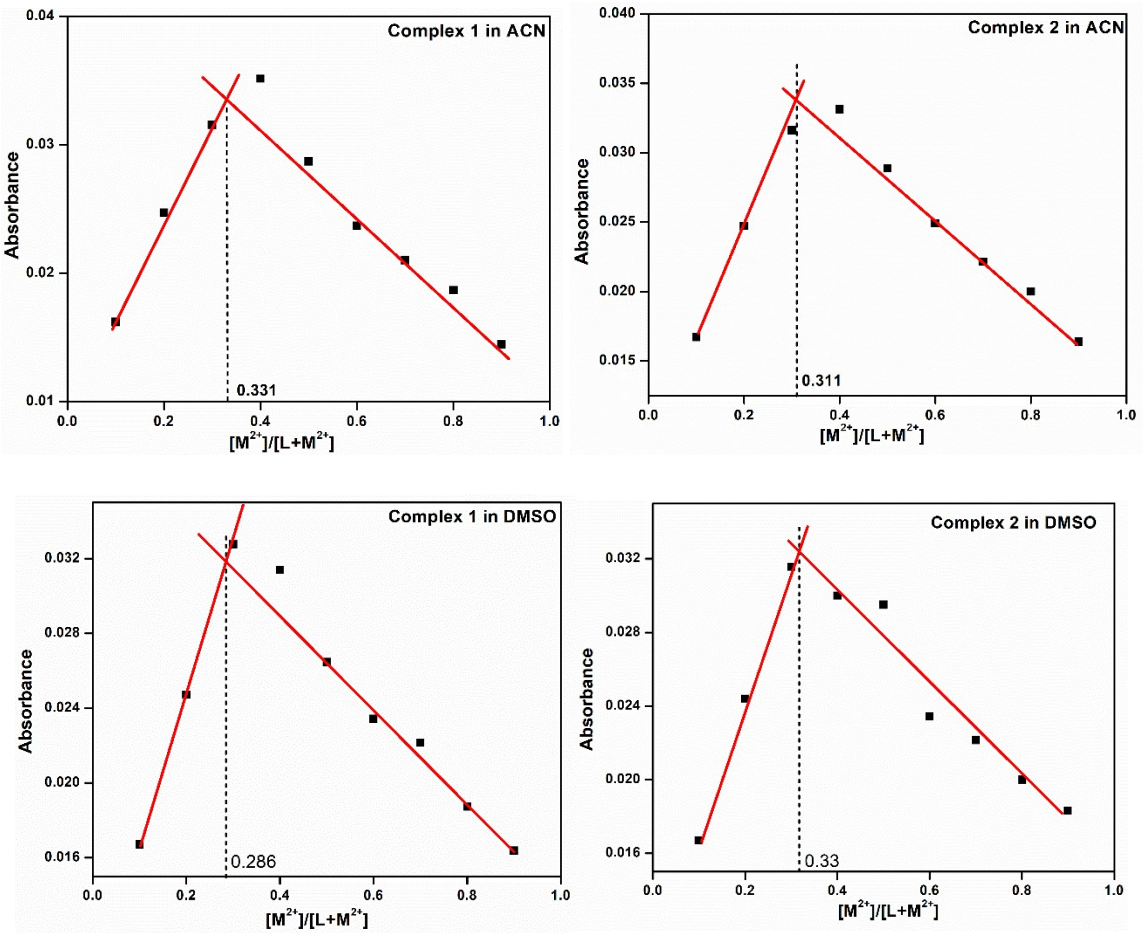

Figure S16: Job's plots for complexes **1-2** in ACN (top) and DMSO (below) medium

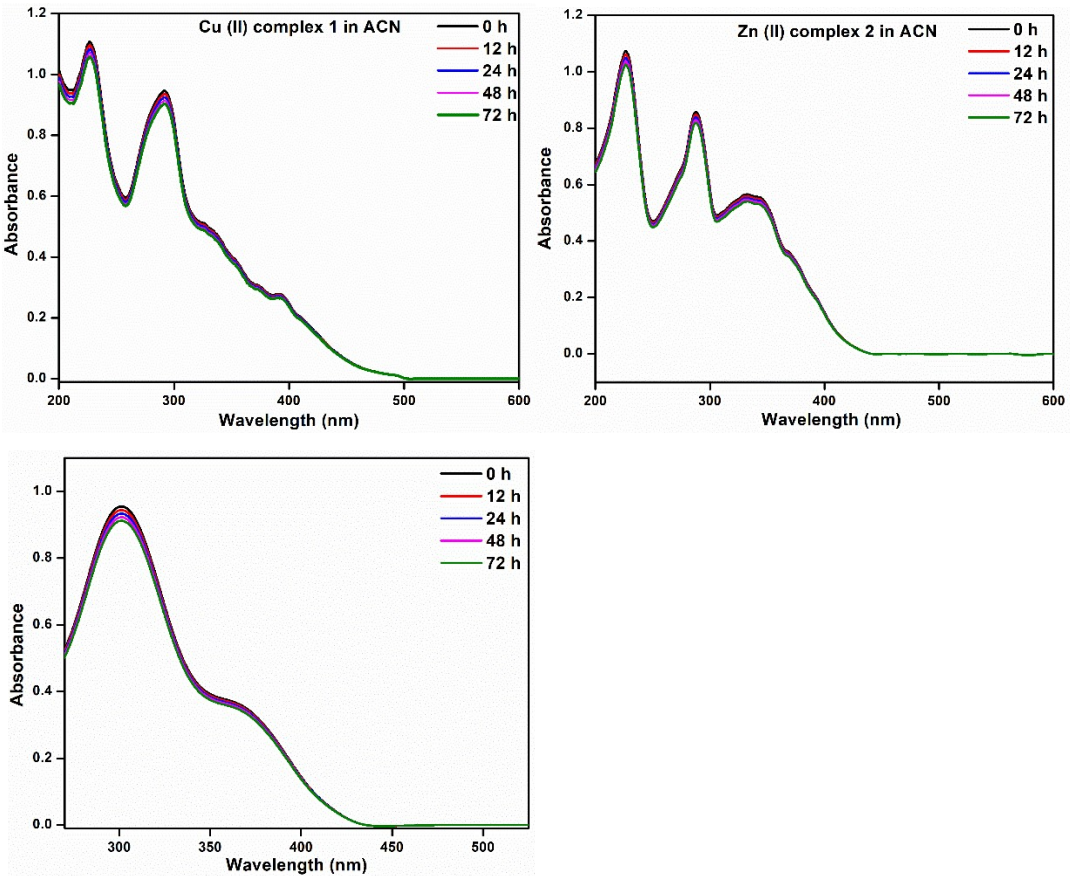

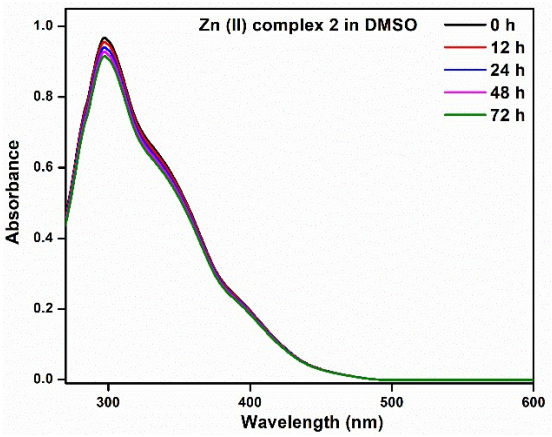

Figure S17: UV-Visible absorption spectra of the complexes 1-2 at different time intervals in ACN (top) and DMSO (below).